water

MDPI

Article

Seasonal Dynamics and Three-Dimensional Hydrographic Features of the Eastern Gulf of Thailand: Insights from High-Resolution Modeling and Field Measurements

Tanuspong Pokavanich [1,*], Vasawan Worrawatanathum [1], Kittipong Phattananuruch [1] and Sontaya Koolkalya [2]

[1] Department of Marine Science, Faculty of Fisheries, Kasetsart University, Bangkok 10900, Thailand
[2] Faculty of Agricultural Technology, Rambhai Barni Rajabhat University, Chanthaburi 22000, Thailand
* Correspondence: ffistop@ku.ac.th

Abstract: Through the integration of high-resolution hydrodynamic modeling and comprehensive field measurements, this study elucidates the intricate three-dimensional hydrographic characteristics of the eastern Gulf of Thailand (eGOT). In addition to the prevalent tidal currents dictating alternating flow along the northwestern and southeastern axes, our investigation reveals pronounced seasonal variations in mean currents, water temperature, and salinity within the eGOT, closely linked to the dynamics of the Asian–Australian monsoon system. During the southwest monsoon, mean currents exhibit a southeasterly trend, contrasting with a northwesterly pattern during the northeast monsoon. Lowest water temperatures occur during the latter, while the highest levels are observed during the 1st monsoon transition (April–March). Notably, salinity levels reach their lowest levels during the southwest monsoon and the 2nd monsoon transition (October), coinciding with the seasonal stratification of the water column and the emergence of a distinct stable along-the-shore northwesterly current with the average speed of 15 cm/s, defined here as the "Chanthaburi Coastal Current (CCC)". Model experiments attribute the formation of the CCC to decreased salinity induced by direct rainfall, highlighting the significance of rainfall as a key factor influencing coastal water dynamics in tropical regions or areas experiencing high precipitation.

Keywords: direct rainfall; Gulf of Thailand; Chanthaburi Coastal Current; monsoon; three-dimensional modeling; salinity dynamics; seasonal variability

Citation: Pokavanich, T.; Worrawatanathum, V.; Phattananuruch, K.; Koolkalya, S. Seasonal Dynamics and Three-Dimensional Hydrographic Features of the Eastern Gulf of Thailand: Insights from High-Resolution Modeling and Field Measurements. *Water* **2024**, *16*, 1962. https://doi.org/10.3390/w16141962

Academic Editor: Georg Umgiesser

Received: 14 May 2024
Revised: 14 June 2024
Accepted: 20 June 2024
Published: 11 July 2024

1. Introduction

The eastern Gulf of Thailand (eGOT), depicted in Figure 1, spans over 25,000 km^2 and constitutes a shallow coastal water body situated at the northeastern extremity of the Gulf of Thailand. With an average depth of 35 m and the deepest area located offshore in the southwestern direction, reaching a maximum depth of 65 m, the eGOT encompasses approximately 500 km of coastline, which represents approximately 15% of Thailand's total coastline. It serves as a crucial site for marine environmental and socio-economic services in Thailand. The sea within the eGOT borders the coastal zones of Rayong, Chanthaburi, and Trat provinces in Thailand, as well as western regions of Cambodia, hosting vital industries, tourism facilities, cities, fisheries, and farmland. Despite its significant footprint, there exists limited documentation regarding its hydrographic characteristics. A comprehensive understanding of the hydrographic properties and their variations is essential for facilitating improved sea and resource management in this region.

Previous hydrographic investigations pertaining to the eastern Gulf of Thailand (eGOT) have predominantly focused on the broader characteristics of the Gulf of Thailand on a regional scale, with the eGOT area being merely a subset of their scope. Notably, ref. [1] utilized data from the NAGA expedition to provide an initial description of the intricate hydrographic dynamics within the South China Sea and the Gulf of Thailand, highlighting their seasonal variability linked to the Asian–Australian monsoon. Subsequent numerical

studies, including those by [2–5] have further elucidated the seasonal variations in Gulf of Thailand circulation. These variations are shown to be influenced by a combination of factors, including tides, prevailing winds, river discharge, direct rainfall to the sea, and sea surface heat exchanges. Ref. [6] conducted an analysis utilizing data obtained from High-Frequency Radar, unveiling seasonal variations in tidal residual surface current patterns. Additionally, ref. [7] corroborated these observations, providing further insight into the intricate complexities of these variations through the utilization of remotely sensed data.

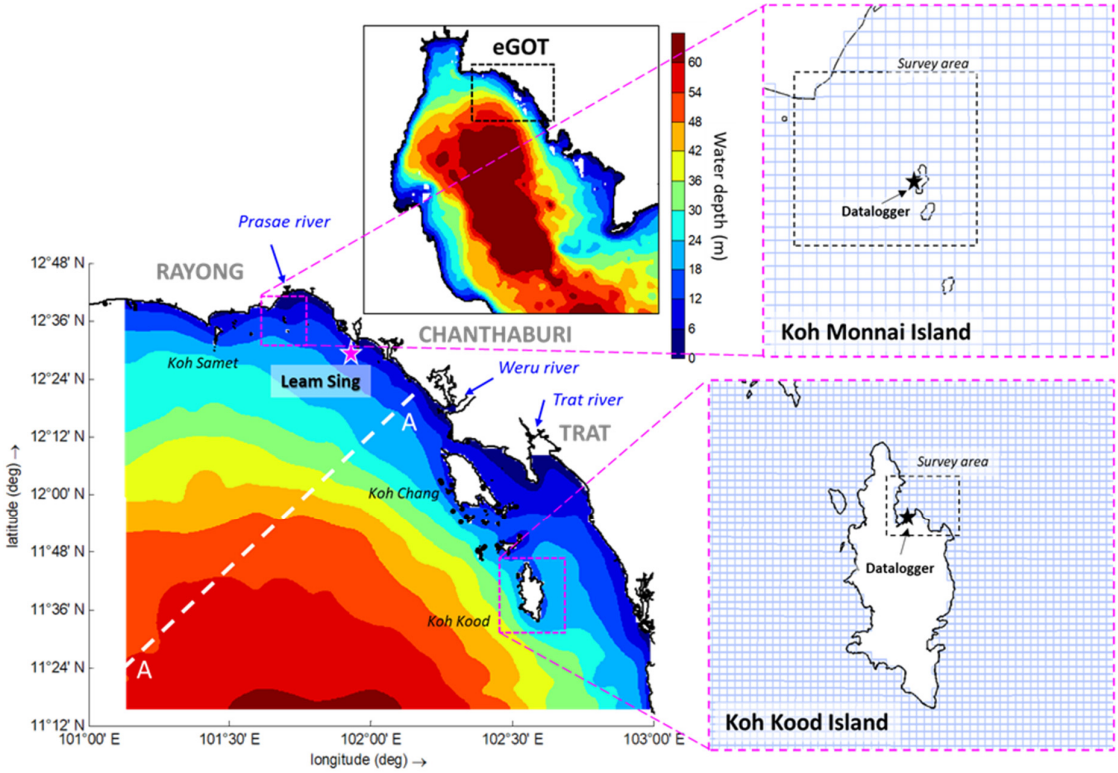

Figure 1. Location map, bathymetry, and modeling domain of the eastern Gulf of Thailand (eGOT) within the larger Gulf of Thailand. Star symbols indicate the locations of field-observed data, while inset plots provide detailed views of the modeling grid and survey areas near Koh Monnai Island and Koh Kood Island. Dashed white line shows location the A-A section.

Early works that provide detailed insights into the eGOT are scarce [8], utilizing remotely sensed observations to discern the presence of a warm water pool during winter in the northeastern region of the Gulf of Thailand, adjacent to the eGOT. This phenomenon was attributed to orographic effects from the Cardamom Mountains in Cambodia. Furthermore, ref. [9] conducted limited field measurements using current meters at Ban Leam Sork in Trat province, revealing robust tidal currents with maximum speeds reaching 24 cm/s. They observed alternating flow directions during flood and ebb tides, along with residual currents predominantly towards the southeastern direction in December. Additionally, they documented the intricate seasonal patterns of residual currents around Trat province. These patterns were found to be influenced by strength of the monsoonal winds, which were further modified by tides and local topography.

Expanding upon previous research, field evidence and unpublished reports have revealed peculiar hydrographic features within the eastern Gulf of Thailand (eGOT). Notably, despite the absence of significant river inflows, instances of low salinity seawater (<28 ppt) have been documented, with notable salinity disparities (>2–3 ppt) between near-surface and sub-surface layers. We hypothesize that this reduced salinity stems from direct rainfall into the sea. Although lacking major river inputs, the eGOT experiences rainfall rates exceeding the national average. Direct rainfall likely diminishes coastal water

salinity, thereby reducing overall water density. Consequently, a freshwater layer can form atop denser seawater, resulting in stratification that hampers vertical mixing and restricts exchanges of heat, nutrients, and dissolved gases between surface and deeper layers. Such stratification may induce buoyancy-driven flows and horizontal currents, influencing coastal hydrodynamics and distinguishing the eGOT from the broader Gulf of Thailand (GOT) system. Similar phenomena of rainfall influence on coastal dynamics have been documented both in the open ocean [10,11] and coastal environments [12–14]. Moreover, studies by [5,15] have demonstrated the substantial impact of atmospheric freshwater fluxes of the Asian–Australian monsoon system on the Bay of Bengal and the Gulf of Thailand, respectively. Alterations in coastal hydrodynamics induced by direct rainfall can yield ecological ramifications. Changes in circulation patterns and stratification can affect nutrient availability, primary production, and the distribution of plankton and other marine organisms, thereby influencing ecosystem dynamics [16–18].

This paper aims to offer detailed insights into the topographic, meteorological and three-dimensional hydrographic characteristics of the eGOT intricate three-dimensional hydrography of the region. Furthermore, we present influence of direct rainfall on local three-dimensional hydrography at the eGOT and the emergence of the Chanthaburi Coastal Current (CCC) through numerical experiments. This finding holds relevance for hydrodynamic modeling endeavors in tropical shallow coastal regions that receive significant freshwater inputs, not only from river systems but also from direct rainfall.

2. Materials and Methods

2.1. Study Site

The eastern Gulf of Thailand (eGOT) comprises a vast coastal expanse spanning Rayong, Chanthaburi, and Trat provinces. Similar in depth to the broader Gulf of Thailand (GOT), the eGOT features average depths of 25 m, with a maximum depth of 65 m offshore. The area has many islands with various sizes, exceeding 50 in total, with notable examples including Koh Samet, Koh Chang, and Koh Kood islands (see Figure 1). Contributing to the hydrology of the eGOT are two medium-sized rivers: the Prasae River, the Weru River, and the Trat River. Over a 15-year period (2006 to 2020), averaged modeled discharge data from the Global Flood Awareness System [19] estimate an annual freshwater discharge from rivers in the eGOT at approximately 7.58 km^3. Compared to the total major river-sourced freshwater for the entire GOT (approximately 57.98 km^3), river-sourced freshwater in the eGOT accounts for only 13%.

Wind data from the ECMWF-ERA5 reanalysis dataset [20] exhibit good agreement with measurements from Thailand's Meteorological Agency stations. Averaged over 15 years, the ECMWF-ERA5 data, as depicted in Figure 2, illustrates the significant influence of the Asian–Australian monsoon system, characterized by two monsoon seasons and two transitional periods. Specifically, the northeast monsoon (NEM) occurs from November to February, the first monsoon transition (Transition 1) from March to April, the southwest monsoon (SWM) from May to September, and the second monsoon transition (Transition 2) in October. To represent these distinct climatic conditions, December, April, August, and October were selected to, respectively, signify the NEM, Transition 1, the SWM, and Transition 2. Wind during monsoons are slightly stronger winds when compared to the relatively calm wind during the monsoon transitions.

Rainfall data indicate non-uniform distribution throughout the year, with higher intensities occurring during the SWM and Transition 2. During these periods, 85% of the total annual direct rainfall into the sea is observed. When consider freshwater input fluxes budget annually, the direct rainfall into the sea (58.0 km^3) significantly surpasses river-sourced freshwater contribution (7.6 km^3), as derived from the GloFAS dataset [19], by a factor of seven. Figure 3 illustrates the detailed seasonal variation in freshwater fluxes to the eGOT.

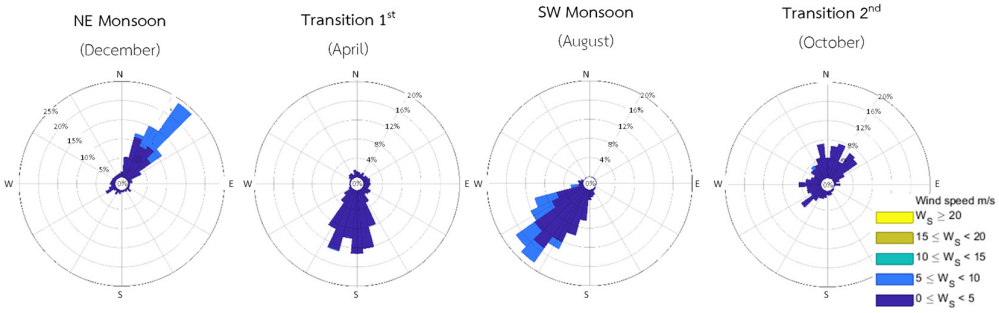

Figure 2. Monthly average wind rose derived from the ECMWF-ERA5 dataset between 2006 and 2020 showing at different monsoonal periods from Koh Monnai Island.

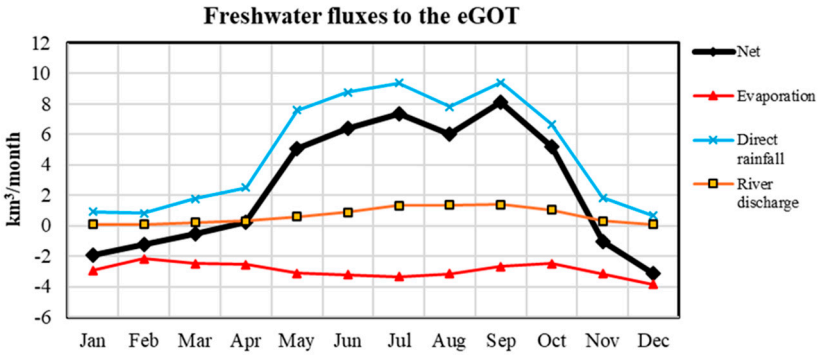

Figure 3. Freshwater fluxes of the eGOT. Data are from the ECMWF-ERA5 reanalysis dataset and the GloFAS dataset averaged monthly between 2006 and 2020.

2.2. Field Observation

Seasonal synoptic measurements were conducted around Koh Monnai Island and Koh Kood Island to collect water temperature and salinity data using a multi-parameter water quality profiling sonde (AAQ-RINKO, JFE Advantech, Kobe, Japan). Additionally, current flow velocity profiles were obtained using an acoustic Doppler current profiler (ADCP) with bottom tracking functionality (Sentinel Workhorse 1200 kHz, Teledyne RD Instrument, San Diego, CA, USA), measuring downward-facing currents. Salinity distribution at various depths around Koh Monnai Island and Koh Kood Island is presented in Figures 4 and 5, respectively. ADCP measurement results at Koh Kood Island are depicted in Figure 6, with the survey area location map provided in Figure 1. The observational sites were sourced from two different study projects. Since both are located in the eGOT, we combined them to represent field data for our study area.

In addition to the seasonal synoptic survey, long-term deployment of dataloggers was undertaken to monitor temporal variations in the water level, water temperature, and salinity at Koh Monnai Island (101°41′10.26″ E, 12°36′48.65″ N) and Koh Kood Island (102°34′13.04″ E, 11°42′20.76″ N). Water depths around Koh Monnai Island range between 4 and 10 m. HOBO-Water level loggers (Onset, MA, USA) and HOBO-Conductivity loggers (Onset, MA, USA) were deployed within perforated PVC pipes at 30 min intervals. Continuous deployment of dataloggers at Koh Monnai Island spanned from October 2019 to November 2021, while deployment at Koh Kood Island lasted for a minimum of 15 days during different monsoon seasons between 2021 and 2022. Local maintenance efforts ensured the quality of observed data by regularly cleaning the loggers. Furthermore, additional water level measurements from the Thailand Hydrographic Department at Leamsing Station (101°57′40.89″ E, 12°27′48.31″ N) were utilized for model validation purposes.

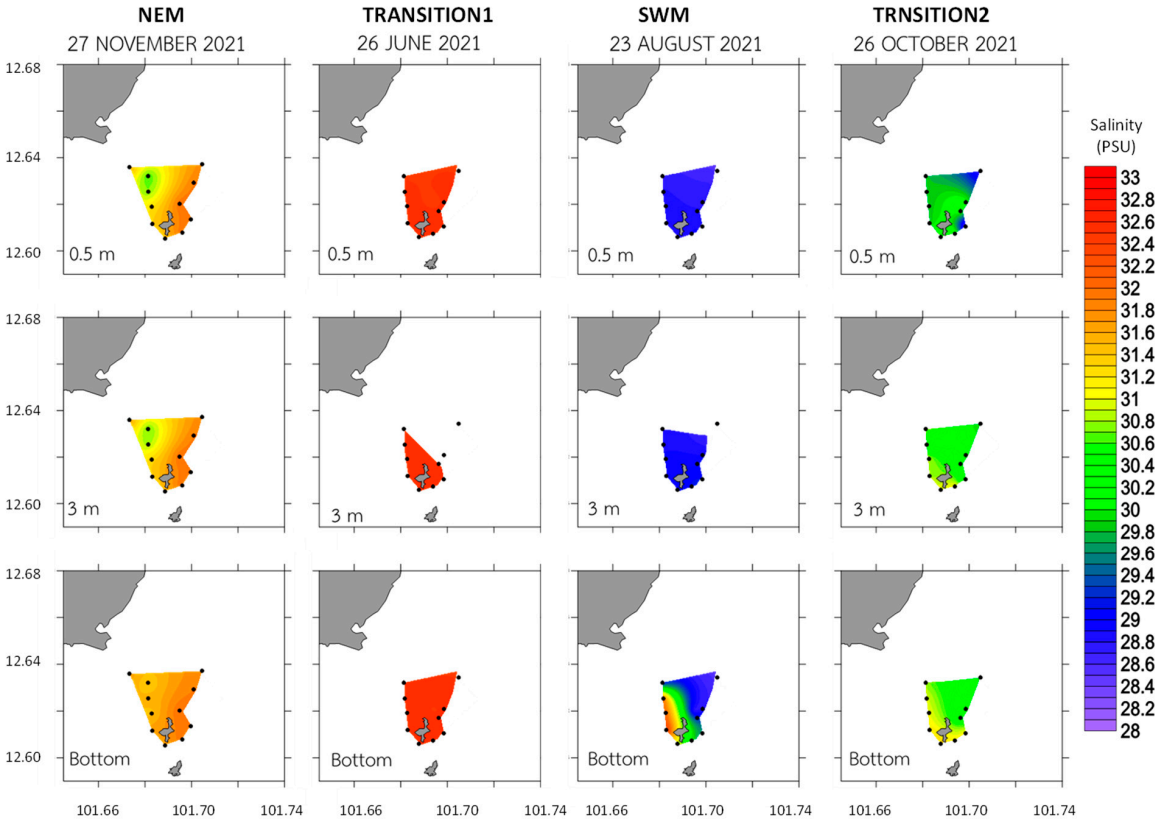

Figure 4. The salinity distribution at various times and depths around Koh Monnai Island was derived from synoptic survey data interpolation. The locations of the measurements are denoted by black dots.

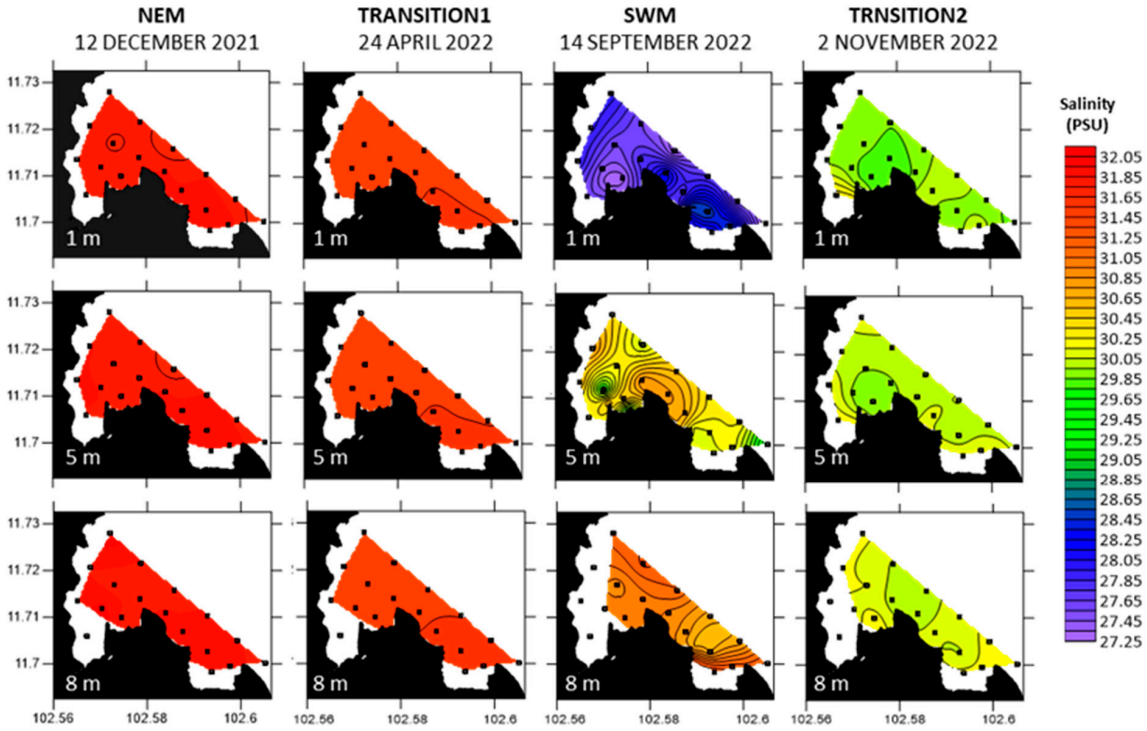

Figure 5. The salinity distribution at various times and depths around Koh Kood Island was derived from synoptic survey data interpolation. The locations of the measurements are denoted by black dots.

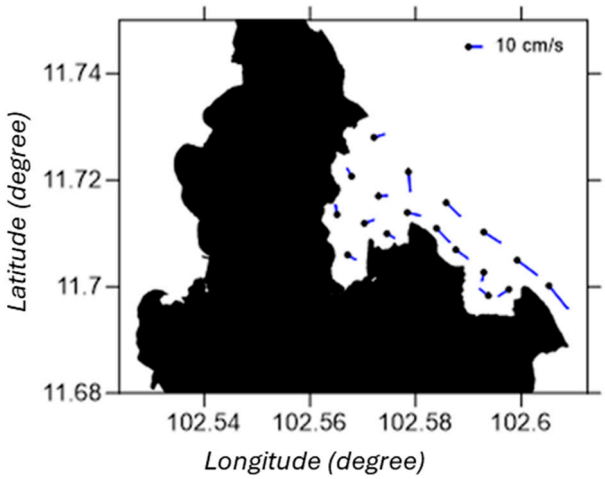

Figure 6. Near-surface flow velocity field from ADCP measurement facing down with bottom tracking functionality at Koh Kood island during ebb tide on 14 September 2022.

2.3. Hydrodynamic Modeling

A three-dimensional hydrodynamic model was established using the Delft3D-FLOW program [21]. The model employs a rectangular grid in spherical coordinates, covering the entirety of the eGOT. It consists of 273 × 326 horizontal grid cells and incorporates 10 vertical layers in sigma coordinate. The thickness of each layer, from surface to bottom, constitutes 2%, 6%, 8%, 10%, 10%, 10%, 10%, 12%, 14%, and 18% of the total water depth, respectively. Simulations encompass a period of one year, from 1 January 2020 to 31 December 2020, capturing all monsoonal fluctuations. Offshore boundary conditions are derived from the whole GOT model, which operates three-dimensionally and includes effects of tides, wind, river discharge, and direct precipitation. The eGOT model is forced with offshore water levels, depth-varying water temperature, and salinity data from the whole GOT model. We also add this important information to the Section 2.3.

The model includes a spin-up time of one year, where the final conditions of the cool start year initiate the warm start of the run. External forcings comprise offshore water level data from the OSU TPXO tide model [22] and layer-varying water temperature and salinity derived from an in-house three-dimensional model of the Gulf of Thailand. Bed shear stress is calculated using a quadratic bed stress formula, with a Chezy bottom roughness number set at 70 m½/s. Meteorological data are sourced from ECMWF-ERA5 reanalysis data at 3 h intervals [20]. The wind drag coefficient follows a quadratic formula [23], with coefficients of 0 and 0.004 at wind speeds of 0 m/s and 25 m/s, respectively. The model utilize k-epsilon turbulent closure model with 10 m^2/s as a background eddy viscosity and eddy diffusivity. Delft3D-FLOW take into account changes in water density from calculated water temperature and salinity using the equation of stage. The water temperature and salinity are calculated using advection and diffusion equation. The model accounts for freshwater fluxes input solely from direct rainfall, as river discharge data contribution is deemed significantly lower in comparison. Amount of the freshwater fluxes is added to the top layer of the model in which mass balances are calculated using conservation of mass equation. Heat fluxes at the water surface is calculated using Ocean Model as a build-in model in the Delft3D-FLOW [24,25] that take into account heat gain from net solar radiation, effective back radiation, heat losses from evaporation and convection. The eGOT is located in a relatively calm sea area with an average wave height of less than 1.0 m, except during the SWM when it slightly increases to less than 1.5 m. Consequently, the impact of waves on the hydrodynamics of this region was disregarded in this study.

3. Results and Discussion

3.1. Field Observation Results

The seasonal spatial distributions of field data are depicted in Figures 4–6, while the temporal variations are illustrated in Figure 7. The temporal data are from dataloggers that are deployed continuously and cover over a year, representing timescales not documented elsewhere. The results reveal daily, tidal, non-tidal longer-term, and seasonal variations in hydrographic conditions. There are significant seasonal fluctuations in water temperature, ranging from 24 to 33 °C. The highest water temperature is observed during Transition 1, contrasting with the lowest temperature recorded during the NEM period. In terms of salinity at Koh Monnai Island, levels range between 26 and 33 PSU, with peak salinity occurring during the NEM season and the lowest during the SWM and Transition 2. Consistent water temperatures and salinities are observed between near-surface and near-bottom layers at Koh Monnai Island and Koh Kood Island, except for the SWM period when near-surface temperatures are warmer/fresher than near-bottom values.

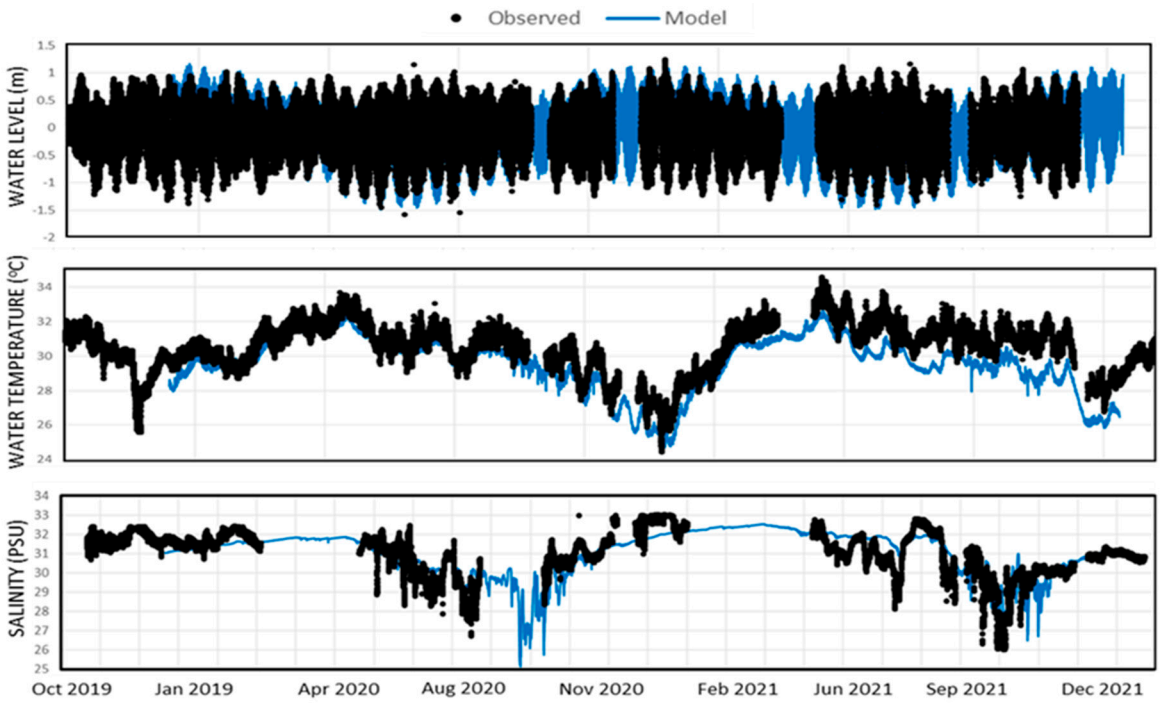

Figure 7. Comparison between continuous measurements of the water level, water temperature, and salinity at Koh Monnai Island and the modeled results. The measurement data are represented by blank dots, while the model results are indicated by a blue line.

Water level data exemplify pronounced tidal fluctuations, with a tidal range of 1–2.5 m during neap and spring tides. Tides are mixed tide prevailing diurnal which governed by M2, S2, O1, P1, K1 tidal. The amplitudes were 0.34, 0.16, 0.53, 0.18, 0.1 m, respectively. The Formzahl number (K1 + P1 + O1)/(M2 + S2) has a value of 1.62. The annual sea level variation in this area, from measured data, is approximately 0.24 m, with the highest average sea level occurring at the start of the year and the lowest in the middle of the year. Additionally, current measurements depict significant tidal variations. Specifically, the current flow field at Koh Kood Island's measurement station during ebb tide reveals a complex pattern, with opposite flow directions near the curved coastline compared to the main southeastward current offshore.

Field observations provide initial insights into the significance of tidal influences and complex coastal topography in the eGOT. Although not included here, spatial flow velocity measurements using ADCP at Koh Kood Island reveal complex alternating flow velocity

patterns across different tidal phases. An example of the measurement during ebb tide is presented in Figure 6.

3.2. Model Validation

Model validation against long-term measured data between October 2019 and December 2021 includes the water level at Leamsing Station, and water temperature and salinity at Koh Monnai Island. The model demonstrates good agreement with the observed water level at Leamsing, with a Root Mean Square Error (RMSE) of <14.8 cm from a tidal range during spring tide of approximately 250 cm and an R^2 value of 0.91. For water temperature, the RMSE is 0.76 °C with an R^2 value of 0.81 (see Figure 7). Salinity levels and trends are also well reproduced by the model. The absence of reported RMSE and R^2 values for salinity is due to concerns regarding the absolute accuracy of the measured salinity data. It is anticipated that while the salinity data can capture long-term variations in this region, there may be inaccuracies present stemming from bio-fouling caused by inadequate maintenance of the HOBO-Conductivity logger deployed in remote area. Frequency analysis of water levels at Koh Monnai Station identifies M2, S2, O1, P1, and K1 as dominant tidal constituents, with amplitudes/phases of 0.34/193, 0.16/340, 0.53/328, 0.18/359, and 0.1/135 m/degrees, respectively. The numerical model similarly reproduces realistic water levels, identifying the same primary constituents with corresponding amplitudes/phases of 0.34/191, 0.15/337, 0.50/325, 0.12/329, and 0.04/113 m/degrees, respectively. Effects of tide and complex coastline topography. The complex alternating flow velocity fields governed by tide and irregular coastline are also well reproduced as seen when compare Figures 6 and 8b.

3.3. Tide and Tidal Currents

Tidal currents play a pivotal role in mobilizing and mixing the entire water column within coastal seas. In the eGOT, tides drive water movement alternately along the coastline in a northwest to southeast axis. During the flood tide, tidal currents flow northwestward, while they shift southeastward during the ebb tide. Tidal currents ease during high and low tides. Maximum tidal current speeds during spring tides range between 0.3 and 0.5 m/s, halving during neap tides. Offshore tidal current speeds generally exceed those near the shoreline, except in channels between land and island and island and island (see Figure 8a). Local shoreline irregularities and bathymetry intricately influence tidal flow patterns. At the lee side of headlands, currents change direction, forming clockwise and counterclockwise eddies, evident in both field measurements (see Figure 5) and well reproduced by modeling (see Figure 8b).

3.4. Water Temperature and Salinity

The results from field observations (Figures 4, 5 and 7) and modeling (Figures 9 and 10) demonstrate good agreement in depicting the spatial and seasonal variability of water temperature and salinity in the eGOT, with ranges spanning between 24 and 30 °C and 29 and 32.5 ppt, respectively. Water temperature is lowest during the NEM, rapidly rising to its annual peak during Transition 1. This temperature fluctuation is most pronounced along the shoreline, where waters are coolest during the NEM and warmest during Transition 1. In contrast, salinity exhibits marked changes during the SWM and Transition 2, with reductions observed along the shoreline, particularly along the coasts of Chanthaburi and Trat provinces. It is important to note that since the model does not account for freshwater input from rivers, the observed reduction in salinity is attributed to direct rainfall into the sea surface.

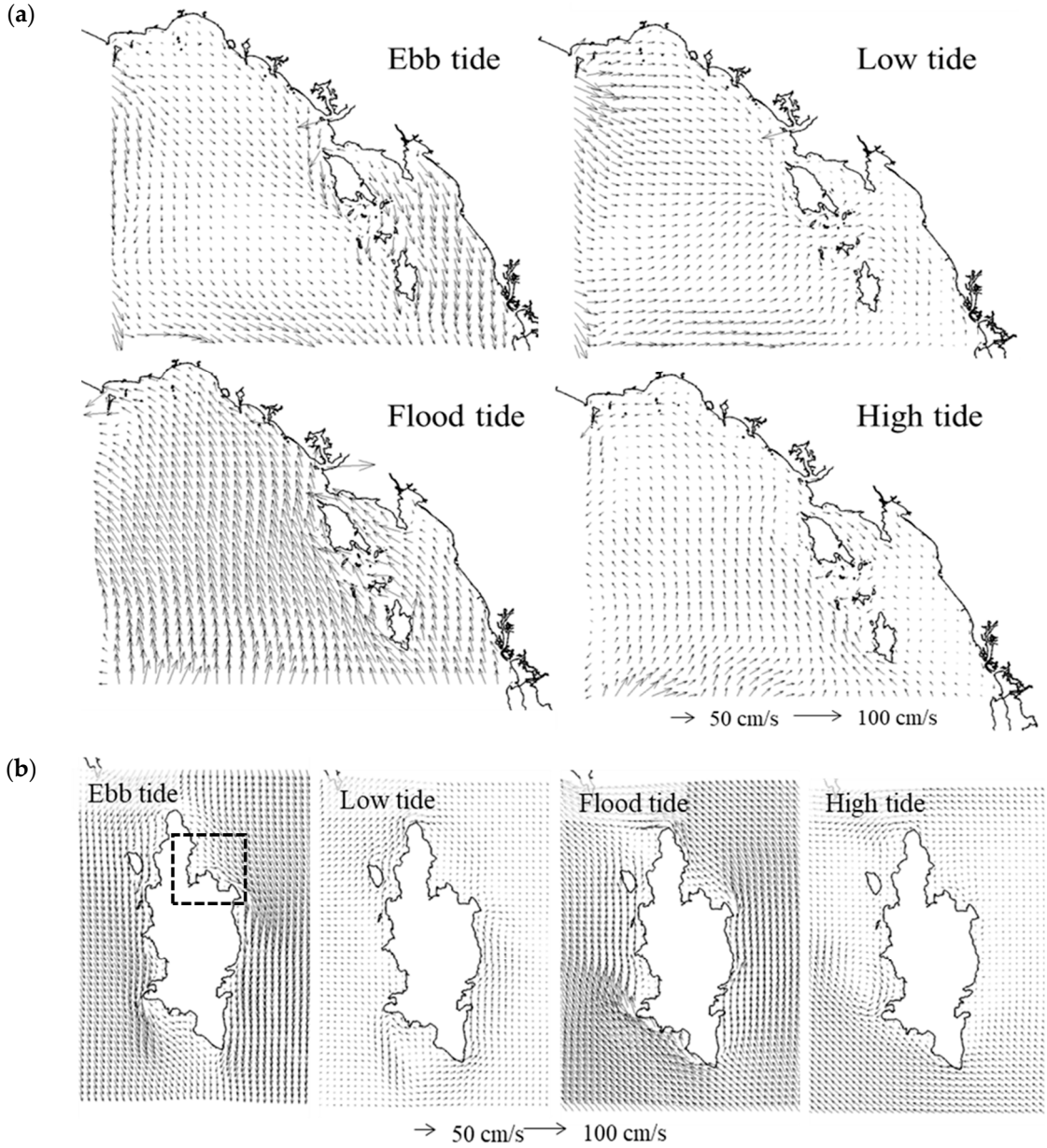

Figure 8. Tidal current patterns (**a**) at the eGOT and (**b**) around Koh Kood Island during spring tide. Dashed line block in (**b**) is the same area of the ADCP measurements.

The model results reveal notable water column stratification characterized by alternating water temperature and salinity profiles. This phenomenon persists throughout the year, except during the NEM when the water column exhibits relatively homogeneous conditions. During Transition 1, a distinct temperature stratification emerges, with the near-surface layer up to 30 m depth exhibiting higher temperatures compared to the lower layers. Following Transition 1, water temperature becomes more evenly distributed throughout the water column. Conversely, salinity does not exhibit significant stratification during Transition 1 but becomes strongly stratified during the SWM and Transition 2. Both water temperature and salinity revert to a more uniform vertical distribution during the NEM.

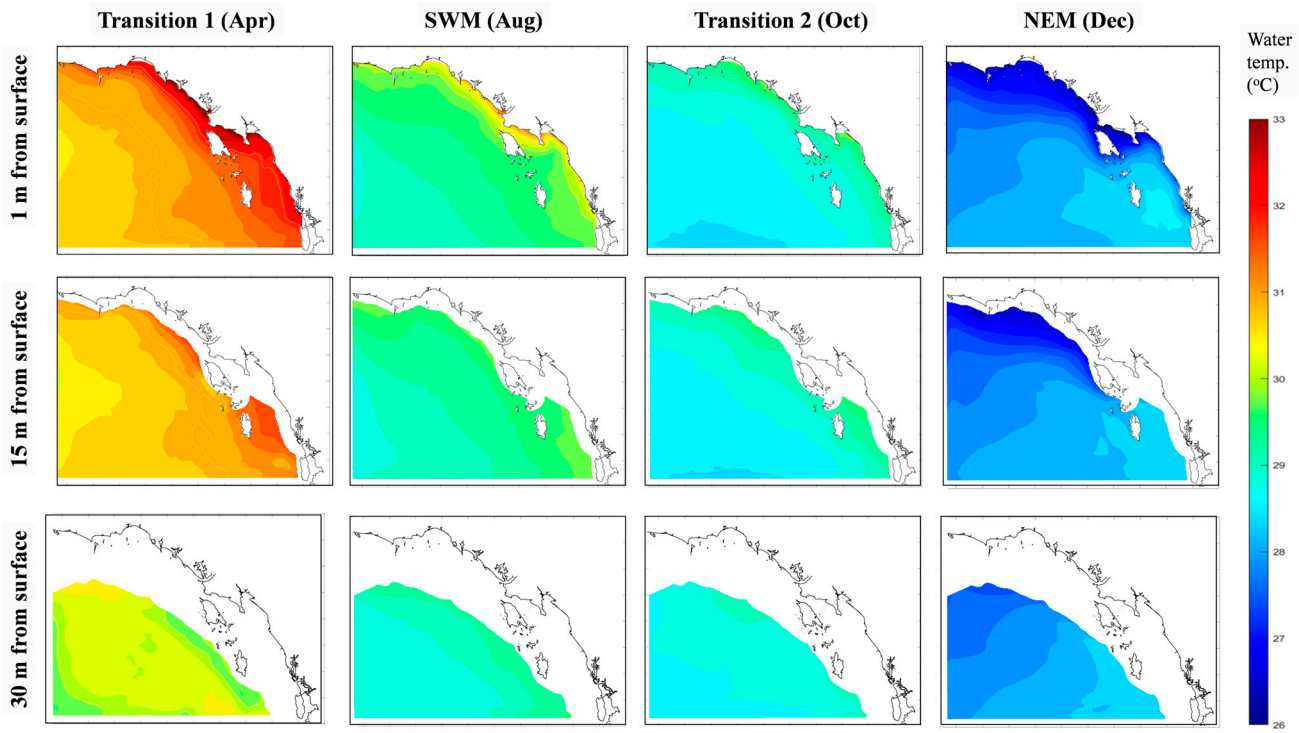

Figure 9. Modeled monthly averaged water temperature at 1 m, 10 m and 20 m from the sea surface at different monsoonal periods.

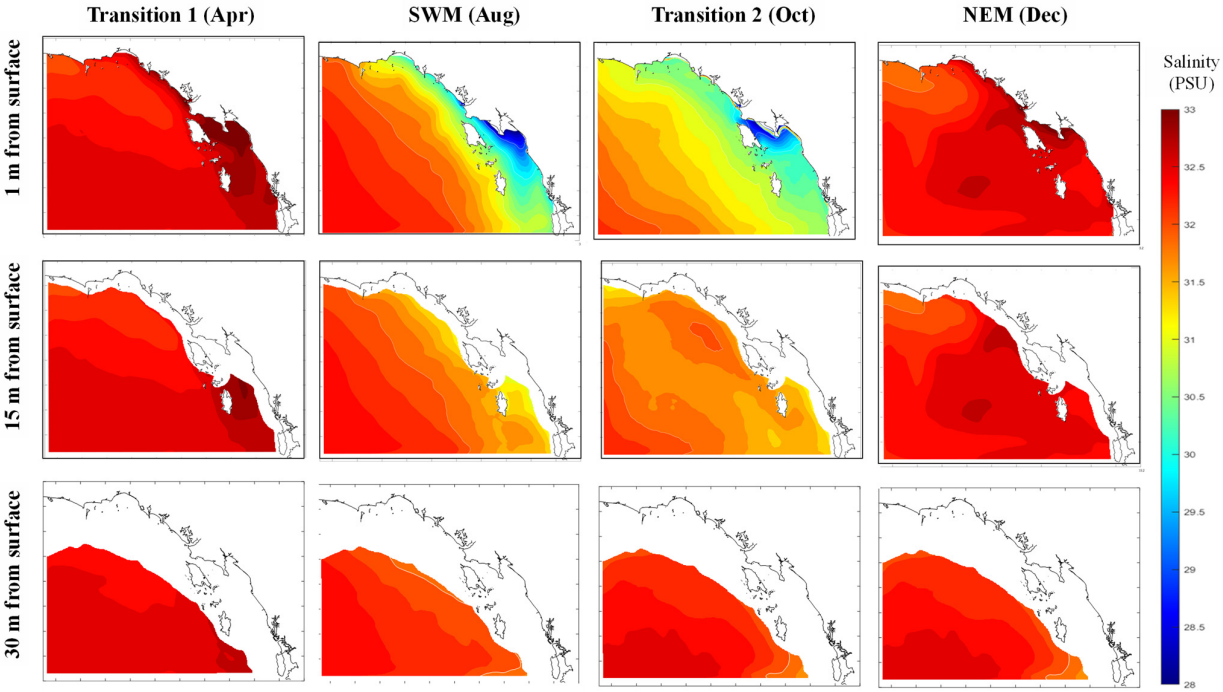

Figure 10. Modeled monthly averaged salinity at 1 m, 10 m and 20 m from the sea surface at different monsoonal periods.

3.5. Seasonal Water Circulation

The monthly mean simulated flow velocity fields depict the diverse circulation patterns of the eGOT influenced by monsoonal effects, as illustrated in Figure 11. Two primary circulation patterns emerge, characterized by flow directions to the southeast during Transition 1 and the SWM, and to the northwest during Transition 2 and the NEM. Monthly

average current speeds peak (>0.15 m/s) during the SWM and the NEM, with the strongest currents observed offshore during the SWM and approximately 40 km from the shoreline during the NEM. Current speeds diminish during the monsoon transitions, albeit with a notable exception during the SWM and Transition 2, where a robust coastal current (within 10 km from the shoreline) flows northeastward with speeds exceeding 15 cm/s. This coastal current, flowing along Chanthaburi Province in Thailand, is dubbed the "Chanthaburi Coastal Current (CCC)" and forms during the SWM, becoming particularly strong and stable during Transition 2.

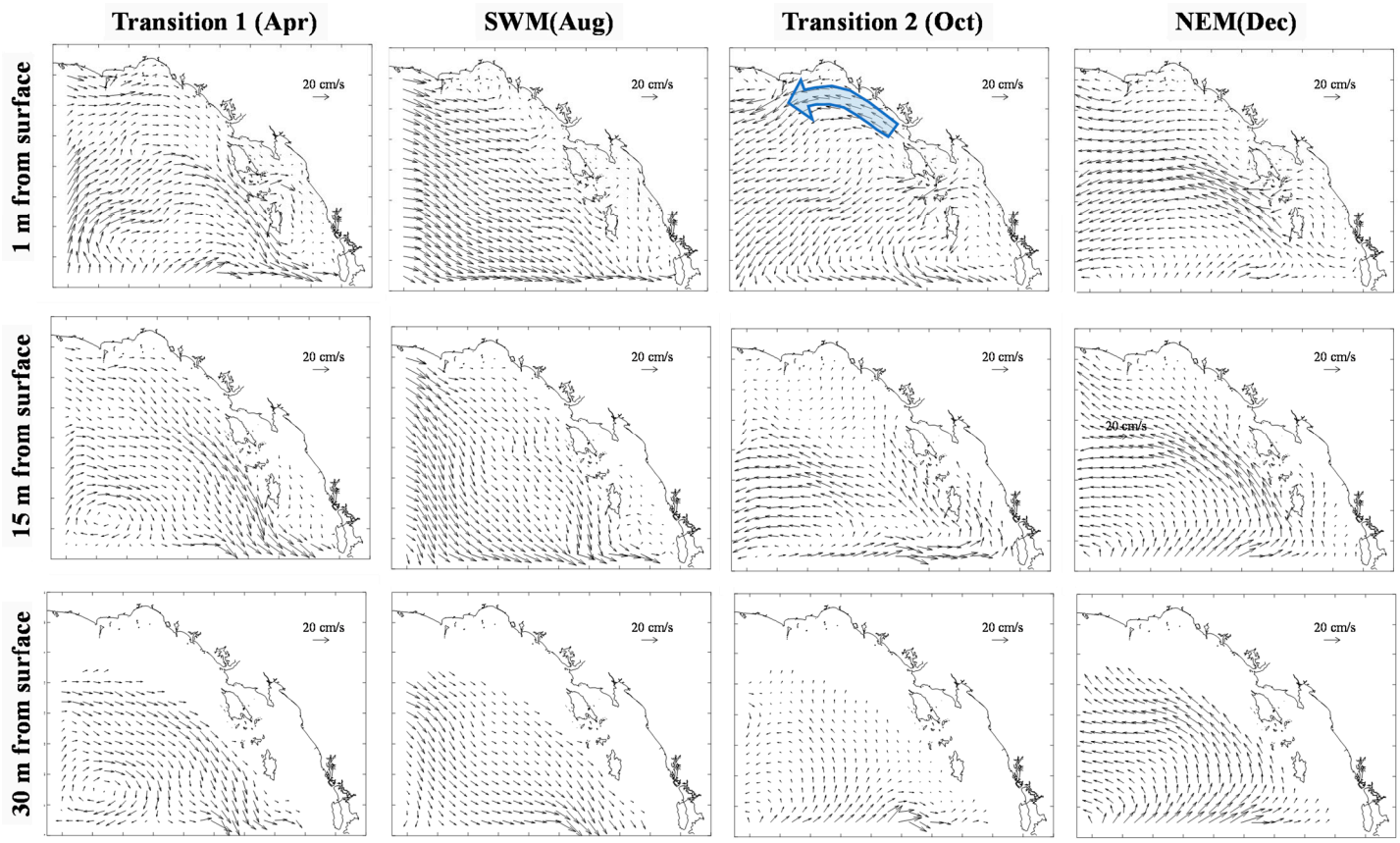

Figure 11. Modeled monthly averaged flow velocity field at 1 m, 15 m and 30 m from the sea surface at different monsoonal periods. Light blue translucent arrows present near-surface values during Transition 2 in the Chanthaburi Coastal Current.

Additionally, the model results highlight significant differences between near-surface and sub-surface circulation, which vary seasonally. Near-surface currents tend to flow towards the land during Transition 1 and the SWM, shifting to offshore flow during Transition 2 and the NEM. Sub-surface counter-currents persist during periods of water column stratification. In Figure 11, averaged current profiles along and across section A-A, location as shown in Figure 1, further elucidate the layered flow patterns during stratified periods, displaying a three-layer and two-layer flow system during the SWM and Transition 2, respectively. Conversely, during the NEM, when the water column is well mixed, flow tends to be more homogeneous.

3.6. Influence of the Direct Rainfall into the Sea

The substantial spatial and temporal variations observed in salinity patterns within the eGOT are expected to exert significant influence on water column dynamics and circulation regimes. Given the prominent role of rainfall in shaping salinity, this study endeavors to explore the impact of direct rainfall through the establishment of an additional model.

Simulations conducted with and without direct precipitation yield insightful outcomes, as depicted in Figures 12 and 13, respectively.

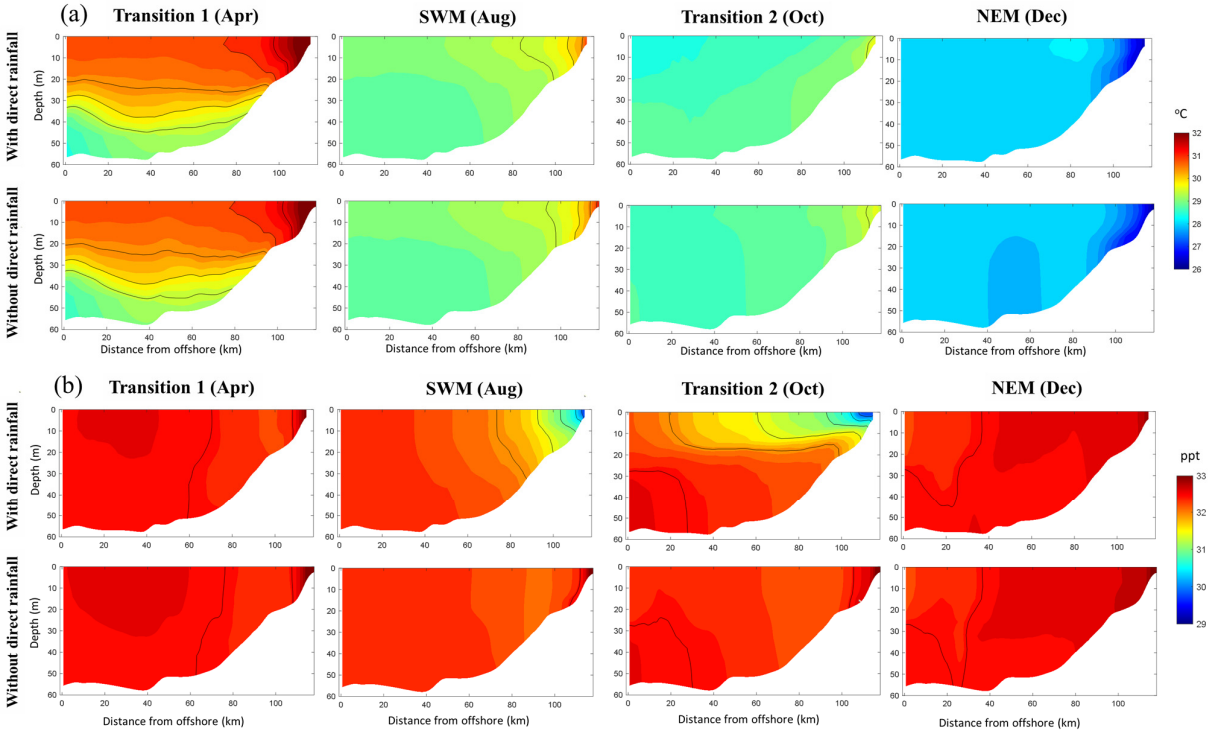

Figure 12. Distribution of the (**a**) water temperature and (**b**) salinity along the A-A section at different monsoonal periods from the model run with and without the direct rainfall into the sea.

A comparative analysis of these outcomes highlights the pronounced effect of direct rainfall, particularly during the SWM and Transition 2 phases, characterized by intensified rainfall and reduced wind activity within the eGOT. While the influence of rainfall on other temporal intervals and water temperature remains relatively subdued, the marked decrease in salinity significantly contributes to water column stratification during the SWM and Transition 2. This stratification profoundly alters overarching circulation patterns, precipitating the emergence of the CCC during these intervals. Notably, the removal of rainfall from the simulations results in the cessation of the CCC and the attendant two-layer circulation.

The influence of freshwater influx from direct rainfall into the marine environment has been previously documented to affect various phenomena, such as the sea surface microlayer [11] and the formation of freshwater lenses under calm wind conditions within the California Current [10]. These effects subsequently exert a notable impact on the hydrodynamic characteristics of the marine domain. Our study marks the first documentation of the effects of direct rainfall on the generation of upper-layer low salinity water, thereby contributing to the genesis of the CCC. Interestingly, a similar occurrence of upper-layer low salinity coastal currents was recently observed during Transition 2 along the western coast of the Gulf of Thailand [26]. However, in that instance, the diminished salinity levels were attributed to river discharge.

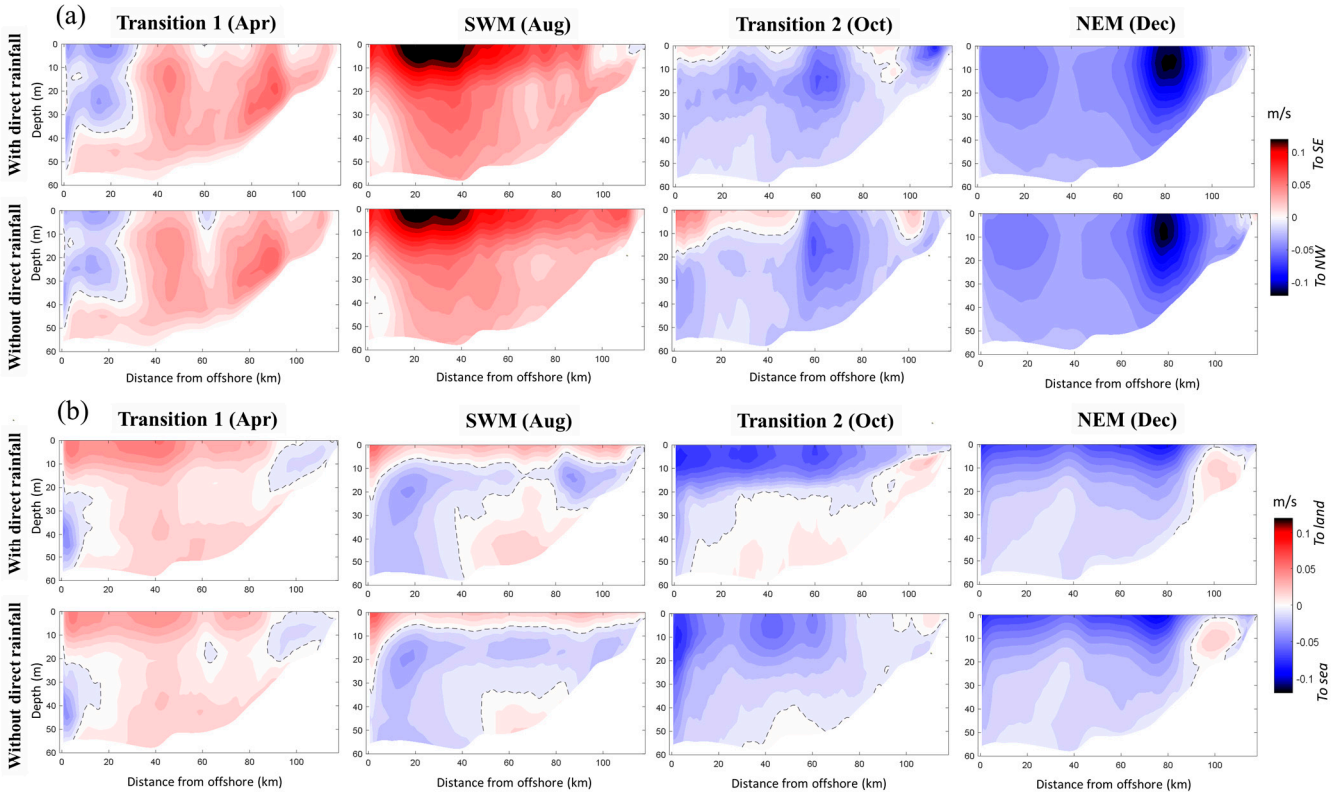

Figure 13. Distribution of the (**a**) monthly averaged flow velocity across the A-A section and (**b**) along the A-A section at different monsoonal periods from the model run with and without the direct rainfall into the sea.

4. Conclusions

Noted from field observations, hydrographic conditions at the eGOT exhibit significant spatial and temporal variability, with pronounced variations in water temperature, salinity, and flow velocities influenced by the Asian–Australian monsoon. Offshore and deep areas typically experience lower water temperatures, reaching their lowest levels during the NEM. During Transition 1, lower layer temperatures are 2–3 degrees lower than near-surface values. The SWM brings higher freshwater input from rainfall, resulting in a significant reduction in the salinity of near-surface layers. This salinity decrease is particularly prominent during the SWM and Transition 2. Differences between near-surface and sub-surface, and near-shore and offshore salinity can be 2–3 ppt, significantly impacting seawater density. The influx of freshwater from rainfall diminishes the overall salinity of coastal waters, leading to decreased water density. During the SWM and Transition 2, strong stratification is observed in shallow areas (water depth < 15 m), influencing coastal hydrodynamics. Salinity levels are low during these periods when rainfall rates significantly increase and wind is relatively calm. Stratification affects vertical mixing and circulation patterns of the water column, altering hydrodynamics. It can hinder vertical mixing and restrict exchange of heat, nutrients, and dissolved gases between surface and deeper layers [10–13,27].

The water circulation in the eGOT exhibits two distinct modes, flowing southeastward during Transition 1 and the SWM, and northwestward during Transition 2 and NEM, closely aligned with predominant wind directions. The strongest circulation occurs during the SWM and NEM periods. Layered flows induced by water column stratification are particularly notable during the SWM and Transition 2. During these periods, a northwesterly Chanthaburi Coastal Current (CCC) emerges. Model simulations suggest that the CCC can be sustained by direct rainfall into the sea during the SWM and Transition 2. The presence of the CCC may significantly influence the seasonal transport of sediments,

nutrients, and pollutants along the eGOT coastline, with ecological ramifications. Altered circulation patterns and stratification affect nutrient availability, primary production, and the distribution of plankton and other marine organisms, ultimately impacting the entire ecosystem and fisheries dynamics [17,18].

Future work is essential to conduct detailed sensitivity analyses and model runs to investigate the mechanisms governing the Chanthaburi Coastal Current (CCC) and its variations. This may include considering freshwater discharges from small rivers and creeks along the eGOT coastline, as well as grid refinement and additional continuous field observations for model validation along the coastline. These efforts could enhance the model's capability to capture the detailed behavior of the CCC. Furthermore, investigation of the effects of changing rainfall patterns in the future, resulting from inter-annual variations in climate drivers such as the El Niño-Southern Oscillation and the Indian Ocean Dipole, is warranted. Additionally, exploring the influence of extreme rainfall events, which are expected to occur more frequently under ongoing global warming, is crucial [14,16,28]. Such future research endeavors will provide valuable insights into the dynamics of the eGOT's hydrographic features and their responses to environmental changes.

Author Contributions: Conceptualization, T.P. and S.K.; methodology, T.P.; software, V.W. and K.P.; validation, T.P., V.W. and K.P.; formal analysis, T.P. and K.P.; investigation, T.P.; resources, T.P. and S.K.; data curation, V.W. and K.P.; writing—original draft preparation, T.P. and V.W.; writing—review and editing, T.P.; visualization, T.P. and K.P.; supervision, T.P.; project administration, T.P. and S.K.; funding acquisition, T.P. and S.K. All authors have read and agreed to the published version of the manuscript.

Funding: This research is a self-funded and partly supported by Agricultural Research Development Agency funded project entitled "Assessment of the releasing effect of the blue swimming crab in the Eastern Gulf of Thailand" (ARDA-POP6405032250). The APC was funded by Faculty of Fisheries, Kasetsart University—Thailand.

Data Availability Statement: Restrictions apply to the datasets.

Conflicts of Interest: The authors declare no conflict of interest.

References

1. Wyrtki, K. *Physical Oceanography of the Southeast Asian Waters*; University of California, Scripps Institution of Oceanography: Berkeley, CA, USA, 1961; Volume 2.
2. Yanagi, T.; Sachoemar, S.I.; Takao, T.; Fujiwara, S. Seasonal variation of stratification in the Gulf of Thailand. *J. Oceanogr.* **2001**, *57*, 461–470. [CrossRef]
3. Aschariyaphotha, N.; Wongwises, P.; Wongwises, S.; Humphries, U.W.; You, X. Simulation of seasonal circulations and thermohaline variabilities in the Gulf of Thailand. *Adv. Atmos. Sci.* **2008**, *25*, 489–506. [CrossRef]
4. Sojisuporn, P.; Morimoto, A.; Yanagi, T. Seasonal variation of sea surface current in the Gulf of Thailand. *Coast. Mar. Sci.* **2010**, *34*, 91–102.
5. Buranapratheprat, A.; Luadnakrob, P.; Yanagi, T.; Morimoto, A.; Qiao, F. The modification of water column conditions in the Gulf of Thailand by the influences of the South China Sea and monsoonal winds. *Cont. Shelf Res.* **2016**, *118*, 100–110. [CrossRef]
6. Saramul, S. Seasonal monsoon variations in surface currents in the Gulf of Thailand revealed by high frequency radar. *Eng. J.* **2017**, *21*, 25–37. [CrossRef]
7. Anutaliya, A. Surface circulation in the Gulf of Thailand from remotely sensed observations: Seasonal and interannual timescales. *Ocean Sci.* **2023**, *19*, 335–350. [CrossRef]
8. Li, J.; Zhang, R.; Ling, Z.; Bo, W.; Liu, Y. Effects of Cardamom Mountains on the formation of the winter warm pool in the gulf of Thailand. *Cont. Shelf Res.* **2014**, *91*, 211–219. [CrossRef]
9. Boonjun, S.; Pransin, M.; Arsiranant, I.; Buranapratheprat, A. The Investigation of Current, Divergence and Convergence in the Coastal Area of Trat Province Using a Hydrodynamic Model. *Burapha Sci. J.* **2023**, *18*, 175–194.
10. Hoffman, L.; Mazloff, M.R.; Gille, S.T.; Giglio, D.; Varadarajan, A. Ocean Surface Salinity Response to Atmospheric River Precipitation in the California Current System. *J. Phys. Oceanogr.* **2022**, *52*, 1867–1885. [CrossRef]
11. Gassen, L.; Esters, L.; Ribas-Ribas, M.; Wurl, O. The impact of rainfall on the sea surface salinity: A mesocosm study. *Sci. Rep.* **2024**, *14*, 6353. [CrossRef]
12. Schmidt, N.; Luther, M.E. ENSO impacts on salinity in Tampa Bay, Florida. *Estuaries* **2002**, *25*, 976–984. [CrossRef]
13. Behara, A.; Vinayachandran, P.; Shankar, D. Influence of rainfall over eastern Arabian Sea on its salinity. *J. Geophys. Res. Ocean.* **2019**, *124*, 5003–5020. [CrossRef]
14. Liu, F.; Zhang, H.; Ming, J.; Zheng, J.; Tian, D.; Chen, D. Importance of precipitation on the upper ocean salinity response to typhoon kalmaegi (2014). *Water* **2020**, *12*, 614. [CrossRef]

15. Haditiar, Y.; Putri, M.R.; Ismail, N.; Muchlisin, Z.; Ikhwan, M.; Ramli, M.; Sugianto Sugianto, R.; Wafdan, M.A.; Rizal, S. The effect of monsoon on the bay of Bengal based on a hydrodynamic model. *J. Eng. Sci. Technol.* **2022**, *17*, 0936–0955.
16. Paerl, H.W.; Valdes, L.M.; Joyner, A.R.; Peierls, B.L.; Piehler, M.F.; Riggs, S.R.; Christian, R.R.; Eby, L.A.; Crowder, L.B.; Ramus, J.S. Ecological response to hurricane events in the Pamlico Sound system, North Carolina, and implications for assessment and management in a regime of increased frequency. *Estuaries Coasts* **2006**, *29*, 1033–1045. [CrossRef]
17. Ballard, T.C.; Sinha, E.; Michalak, A.M. Long-term changes in precipitation and temperature have already impacted nitrogen loading. *Environ. Sci. Technol.* **2019**, *53*, 5080–5090. [CrossRef]
18. Han, H.; Xiao, R.; Gao, G.; Yin, B.; Liang, S. Influence of a heavy rainfall event on nutrients and phytoplankton dynamics in a well-mixed semi-enclosed bay. *J. Hydrol.* **2023**, *617*, 128932. [CrossRef]
19. Harrigan, S.; et al. River discharge and related historical data from the Global Flood Awareness System, v2. 1, Copernicus Climate Change Service (C3S) Climate Data Store (CDS). 2019.
20. Hersbach, H.; Bell, B.; Berrisford, P.; Biavati, G.; Horányi, A.; Muñoz Sabater, J.; Nicolas, J.; Peubey, C.; Radu, R.; Rozum, I. ERA5 Hourly Data on Pressure Levels from 1979 to Present. Copernicus Climate Change Service (C3S) Climate Data Store (CDS). 2018.
21. Deltares. User Manual of Delft3D-FLOW—Simulation of Multi-dimensional Hydrodynamic Flows and Transport Phenomena, Including Sediments. 2003, p.497.
22. Egbert, G.D.; Erofeeva, S.Y. Efficient inverse modeling of barotropic ocean tides. *J. Atmos. Ocean. Technol.* **2002**, *19*, 183–204. [CrossRef]
23. Smith, S.D.; Banke, E.G. Variation of the sea surface drag coefficient with wind speed. *Q. J. R. Meteorol. Soc.* **1975**, *101*, 665–673. [CrossRef]
24. Gill, A.E. *Atmosphere-Ocean Dynamics*; Vol.30 of International Geophysics Series; Academic Press: Cambridge, MA, USA, 1982.
25. Lane, A. *The Heat Balance of the North Sea*; Tech. Rep. 8; Proudman Oceanographic Laboratory: Liverpool, UK, 1989.
26. Pokavanich, T.; Phattananuruch, K. Seasonal hydrographic patterns of the Gulf of Thailand and interactions with the South China Sea: Insights from a numerical Model utilizing the novel dataset. In Proceedings of the 2nd UN Ocean Decade Regional Conference and 11th IOC-WESTPAC Conference, Bangkok, Thailand, 22–25 April 2024.
27. Royer, T.C. On the effect of precipitation and runoff on coastal circulation in the Gulf of Alaska. *J. Phys. Oceanogr.* **1979**, *9*, 555–563. [CrossRef]
28. Donat, M.G.; Lowry, A.L.; Alexander, L.V.; O'Gorman, P.A.; Maher, N. More extreme precipitation in the world's dry and wet regions. *Nat. Clim. Chang.* **2016**, *6*, 508–513. [CrossRef]